

Pt-coated InN nanorods for selective detection of hydrogen at room temperature

O. Kryliouk, H. J. Park, H. T. Wang, B. S. Kang, T. J. Anderson, and F. Ren
Department of Chemical Engineering, University of Florida, Gainesville, Florida 32611

S. J. Pearton^{a)}
Department of Materials Science and Engineering, University of Florida, Gainesville, Florida 32611

(Received 20 May 2005; accepted 27 June 2005; published 15 August 2005)

Single crystal InN nanorods were successfully grown on *c*-Al₂O₃ by hydride-metalorganic vapor phase epitaxy. The measured resistance of bare InN nanorods does not change upon exposure to hydrogen ambient. The addition of sputter-deposited clusters of Pt onto the surface of the InN nanorods, however, produced a significant change in the measured room temperature resistance. The measured resistance changed systematically by 0.5%–12% as the ambient hydrogen concentration in N₂ was varied between 10 and 250 ppm after 15 min exposure time. Importantly, a relatively low power consumption of ~0.3 mW was measured under these conditions. There was no response at room temperature to O₂, N₂O, or NH₃ exposures. © 2005 American Vacuum Society.
[DOI: 10.1116/1.2008268]

I. INTRODUCTION

The growth of one-dimensional semiconductors such as nanowires and nanorods has become a subject of intensive research.^{1–6} InN is currently receiving attention because of its recently reported considerably narrower direct band gap (0.7–0.8 eV)^{7,8} and superior electron transport characteristics.⁹ This makes it a promising material for high efficiency IR emitters, detectors, and solar cells as well as high frequency electronic devices. Reports on the growth, properties, and applications of InN nanorods or nanowires, however, are very limited.^{3–6}

Deposition of InN by conventional metalorganic chemical vapor deposition is challenging because the low thermal decomposition temperature $T \sim 600$ °C under nitrogen pressure of 760 Torr leads to indium droplet formation. Coupling this property to the low rate of decomposition of NH₃ at this temperature, InN growth requires an extremely high NH₃/TMIn ratio.¹⁰ Decomposition of excess NH₃, however, produces H₂, which reduces InN to considerably decrease the InN growth rate. This makes the growth of nanorods or nanowires difficult because their size control will be limited. It is well known that In metal is easily vapor phase etched by reaction with HCl to form volatile InCl and, at lower temperature, InCl₃. Initial complex chemical equilibrium simulation of In-N-H-Cl system suggested InN films could be grown without In droplet formation at low N/In ratio by deposition in a chlorine containing ambient. The calculated results were subsequently confirmed by experiment.¹¹ The results point to the suitability of hydride-metalorganic vapor phase epitaxy (H-MOVPE)¹² to grown InN at low NH₃/TMIn ratio at high rate without In droplet formation.

There is considerable interest in the development of robust, hydrogen-selective sensors for use with proton-exchange membrane and solid oxide fuel cells for space craft

and other long-term sensing applications. These sensors are required to selectively detect hydrogen at room temperature with minimal power consumption and weight. The high surface to volume ratio of nanorods and nanotubes renders them potential candidates for this type of sensing. Several groups have reported applying carbon nanotubes (CNTs) to hydrogen sensing. Pd doping of films or loading with Pd nanoparticles has been used to functionalize the nanotube surfaces to promote catalytic dissociation of H₂.^{13,14} ZnO nanowires and nanorods have also shown potential for use in gas, humidity, and chemical sensing.^{15–17} Although these prior demonstrations of nanorod-based chemical sensors are promising, several issues remain, including quantifying the sensitivity, improving detection limits at room temperature, and reducing power consumption.

In this study, a bed of InN nanorods was grown by H-MOVPE. The InN nanorods were characterized by scanning electron microscopy (SEM), Auger electron spectroscopy (AES), x-ray diffraction, and grazing incidence-angle x-ray diffraction (GIXD). The nanorods were then used for selective detection of hydrogen at room temperature using Pt coatings to promote H₂ dissociation. The sensors are shown to detect ppm level hydrogen at room temperature using ~0.3 mW of power.

II. EXPERIMENT

InN nanorods were grown on polished *c*-Al₂O₃ substrates by H-MOVPE. In this process TMIn is first reacted with HCl in the source zone of the hot-wall reactor to form chlorinated indium species. This stream is then combined with NH₃ in the downstream mixing zone and directed toward the substrate where deposition of InN occurs by reaction of InCl_{*x*} with NH₃. To prevent TMIn decomposition before reacting with HCl, the source zone temperature was maintained below 300 °C. The growth was performed at atmospheric pressure in N₂ ambient (4 slm liquid N₂ boil-off) in the tempera-

^{a)}Electronic mail: speart@mse.ufl.edu

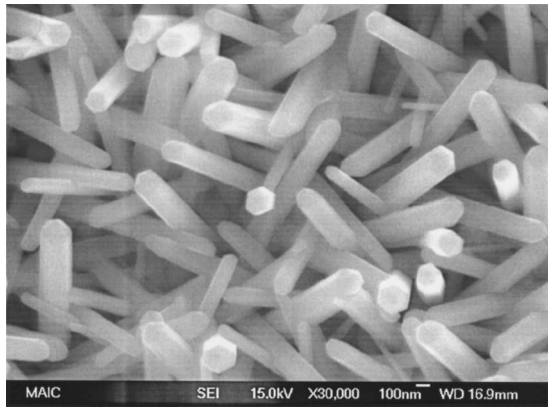


FIG. 1. SEM image of InN nanorods on *c*-Al₂O₃ by H-MOVPE at *T* = 600 °C, HCl/III=5, V/III=250.

ture range 600–650 °C at N/In mole ratio of 250 and HCl/TMIn inlet mole ratio of 4 to 5. TMIn™ from Epichem, Grade5 (99.999 %) NH₃ from Matheson Tri Gas, and HCl were used as precursors. A more detailed description of the H-MOVPE reactor and growth process is presented elsewhere.¹²

Figure 1 shows a SEM micrograph of the as-grown InN nanorods in which a high density of nanorods is produced with a diameter in the range of a few nm to 100 nm. A GIXD scan (Fig. 2) of the InN nanorods on *c*-Al₂O₃ was performed using a Phillips X'Pert system. Since the orientation of each nanorod was largely random, all the wurtzite InN peaks were observed. Based on the AES results shown in Fig. 3, it is concluded that the nanorods are composed of indium and nitrogen, and no chlorine was detected. Selected area diffraction patterns confirmed that the nanorods are single-crystal, while energy dispersive x-ray spectroscopy (EDS) analysis indicated that they are composed of indium and nitrogen, and no chlorine or carbon was detected. The source of oxygen and carbon shown in the AES result in Fig. 3 is believed to be from postgrowth handling of the sample in the air prior to AES characterization. A more detailed presentation of the growth process and their properties is presented elsewhere.¹⁸

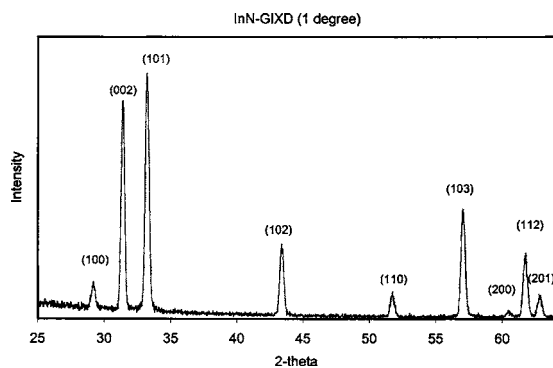


FIG. 2. GIXD 2θ scan of InN nanorods on *c*-Al₂O₃ substrates. Miller indices of hexagonal InN are placed above the corresponding peaks. Incident beam angle = 1°.

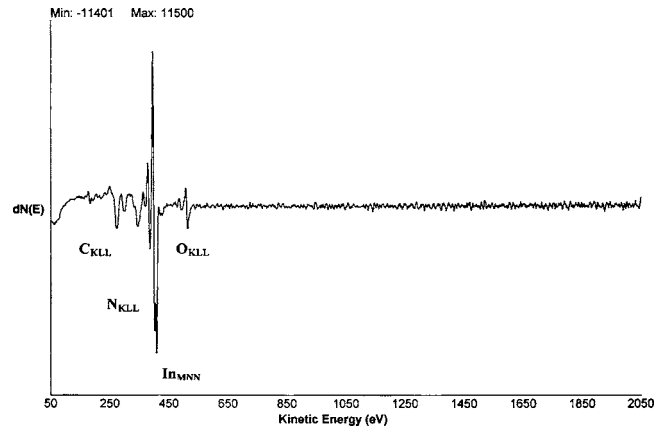


FIG. 3. AES of InN nanorods grown on *c*-Al₂O₃ substrate by H-MOVPE at *T* = 600 °C, HCl/III=5, V/III=250.

In selected samples, the nanorods were coated with thin Pt films (~ 100 Å thick) deposited by sputtering. A shadow mask was used to pattern sputtered Al/Ti/Au electrodes contacting both ends of multiple nanorods on the Al₂O₃ substrates. The separation of the electrodes was ~ 30 μm. Au wires were bonded to the contact pad for current-voltage (*I*-*V*) measurements performed at 25 °C in a range of ambient (N₂, O₂, N₂O, ND₃ or 10 to 250 ppm H₂ in N₂). Note that no underlying thin film of InN was observed for the growth conditions used to grow the tested nanorods.

III. RESULTS AND DISCUSSION

The *I*-*V* characteristics from the uncoated multiple nanorods were linear with typical currents of <0.6 mA at an applied bias of 0.5 V, as shown in Fig. 4. After Pt coatings, the resistance of the nanorods was slightly higher. This may be due to the introduction of sputter damage that decreases the conductivity of the nanorods. We have observed similar effects in ZnO nanorods coated with Pt. The current for the uncoated nanorods was not affected by the measurement ambient, i.e., they showed no response to hydrogen.

Figure 5 shows the time dependence of current (top) or relative resistance change (bottom) of the Pt-coated multiple

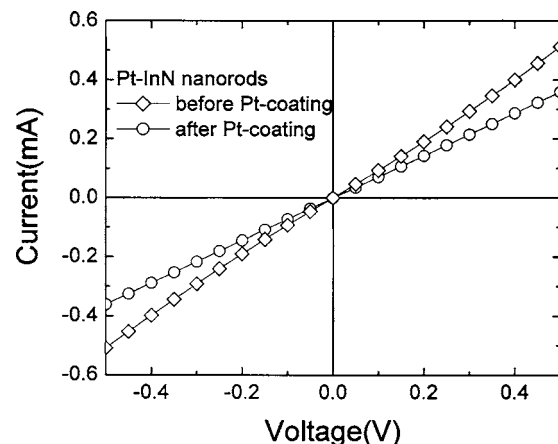


FIG. 4. *I*-*V* characteristics from uncoated and Pt-coated InN nanorods.

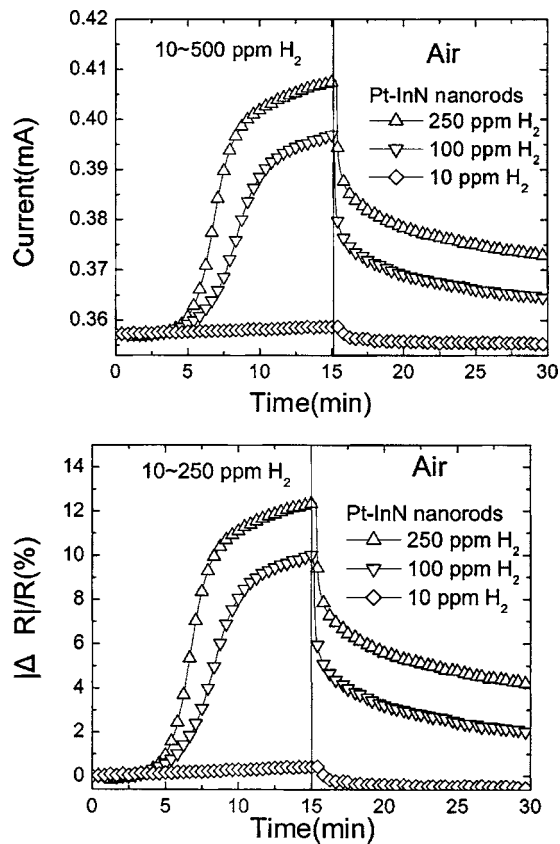


FIG. 5. I -time plot of 10–250 ppm H₂ test by Pt-InN nanorods (top) and $|\Delta R|/R(\%)$ -time plot of 10–250 ppm H₂ test by Pt-InN nanorods (bottom).

InN nanorods as the gas ambient is switched from N₂ to various concentrations of H₂ in air (10–250 ppm) and then back to air as time proceeds. There are several aspects of the data. Note that the addition of the Pt coating on the nanorods now produces a strong response to the presence of hydrogen. The addition of the Pt appears to be effective in catalytic dissociation of the H₂ to atomic hydrogen. There was no response of either type of nanorod to the presence of O₂ in the ambient at room temperature. The nanorod resistance is still changing at least 15 min after the introduction or removal of the hydrogen. The resistance change during the exposure to hydrogen was slower in the beginning and the rate resistance change reached a maximum at ~ 15 min of exposure time. This could be due to some of the Pt becoming covered with native oxide which is removed by exposure to hydrogen. Since the available surface Pt for catalytic chemical absorption of hydrogen increased after the removal of oxide, the rate of resistance change increased. However, the Pt surface gradually saturated with the hydrogen and the rate of resistance change decreased. The reversible chemisorption of reactive gases at the surface of nitrides and oxides can produce a large and reversible variation in the conductance of the material.¹⁹ The relative response of the Pt-coated nanorods was a strong function of H₂ concentration in N₂. The Pd-coated InN nanorods detected hydrogen down to 10 ppm, with relative responses of $\sim 10\%$ at 100 ppm and 12% at 250 ppm H₂ in N₂ after 15 min exposure, as shown in Fig. 5. The

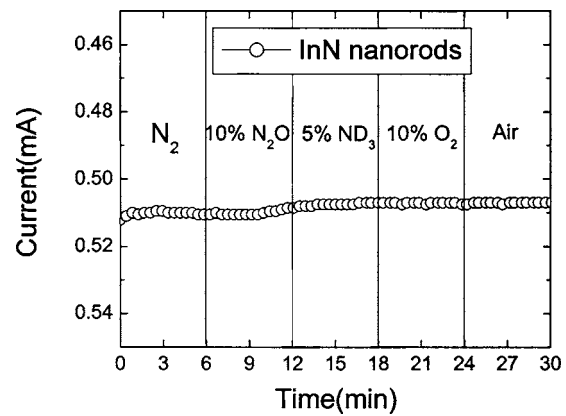


FIG. 6. N₂, N₂O, ND₃, and O₂ test for InN nanorods.

gas sensing mechanisms suggested in the past for semiconductors include the desorption of adsorbed surface hydrogen and grain boundaries in polycrystalline materials,²⁰ exchange of charges between adsorbed gas species and the surface leading to changes in depletion depth,²¹ and changes in surface or grain boundary conduction by gas adsorption/desorption.²² The detection mechanism is still not firmly established in these devices and needs further study. In addition, hydrogen introduces a shallow donor state in InN and this change in near-surface conductivity may also play a role.²³

Figure 6 shows the time dependence of resistance change of Pt-coated InN nanorods as the gas ambient is switched from vacuum to N₂, oxygen, nitrous oxide or ammonia (using the deuterated version) and then back to air. The data confirm the absence of sensitivity to O₂. The rate of resistance change for the nanorods exposed to the 250 ppm H₂ in N₂ was measured at different temperatures. An activation energy of ~ 12 kJ/mol was calculated from the slope of the Arrhenius plot. This value is larger than that of a typical diffusion process. Therefore the dominant mechanism for this sensing process is more likely to be the chemisorption of hydrogen on the Pd surface. Moreover, the data were recorded at a power level of ~ 0.3 mW, which is low even in comparison with CNTs.^{13,14} This is attractive for long-term hydrogen sensing applications.

IV. SUMMARY AND CONCLUSIONS

In conclusion, single crystal InN nanorods were successfully grown by H-MOVPE. Pt-coated InN nanorods appear well-suited to detection of ppm concentration levels of hydrogen at room temperature. The InN nanorods can be placed on cheap transparent substrates such as glass, making them attractive for low-cost sensing applications. Furthermore, it was demonstrated that they can operate at very low power conditions.

ACKNOWLEDGMENTS

The work at UF is partially supported by NSF(CTS-0301178, monitored by Dr. M. Burka and Dr. D. Senich), by NASA Kennedy Space Center Grant No. NAG 10-316 monitored by Daniel E. Fitch, ONR (N00014-98-1-02-04, H. B. Dietrich), and NSF DMR 0400416.

- ¹M. H. Huang, S. Mao, H. Feick, H. Q. Yan, Y. Y. Wu, H. Kind, E. Weber, R. Russo, and P. D. Yang, *Science* **292**, 1897 (2001).
- ²J. C. Johnson, H. Q. Yan, R. D. Schaller, P. B. Petersen, P. D. Yang, and R. J. Saykally, *Nano Lett.* **2**, 279 (2002).
- ³O. Briot, B. Maleyre, S. Ruffenach, C. Piquier, F. Demangeot, and J. Frandon, *Phys. Status Solidi C* **0**, 2851 (2003).
- ⁴E. Dimakis, G. Konstantinidis, K. Tzagaraki, A. Adikimenakis, E. Iliopoulos, and A. Georgakilas, *Superlattices Microstruct.* **36**, 497 (2004).
- ⁵Z. H. Lan, W. M. Wang, C. L. Sun, S. C. Shi, C. W. Hsu, T. T. Chen, K. H. Chen, C. C. Chen, Y. F. Chen, and L. C. Chen, *J. Cryst. Growth* **269**, 87 (2004).
- ⁶T. Tang, S. Han, W. Jin, X. Liu, C. Li, D. Zhang, C. Zhou, B. Chen, J. Han, and M. Meyyapan, *J. Mater. Res.* **19**, 423 (2004).
- ⁷V. Yu. Davydov, A. A. Klochikhin, V. V. Emtsev, D. A. Kurdyukov, S. V. Ivanov, V. A. Vekshin, F. Bechstedt, J. Furthmüller, J. Aderhold, J. Graul, A. V. Mudryi, H. Harima, A. Hashimoto, A. Yamamoto, and E. E. Haller, *Phys. Status Solidi B* **234**, 787 (2002).
- ⁸J. Wu, W. Walukiewicz, K. M. Yu, J. W. Ager III, E. E. Haller, H. Lu, W. J. Schaff, Y. Saito, and Y. Nanishi, *Appl. Phys. Lett.* **80**, 3967 (2002).
- ⁹S. K. O'Leary, B. E. Foutz, M. S. Shur, U. V. Bhapkar, and L. F. Eastman, *J. Appl. Phys.* **83**, 826 (1998).
- ¹⁰Y. Kumagai, J. Kikuchi, Y. Matsuo, Y. Kangawa, K. Tanaka, and A. Koukitu, *J. Cryst. Growth* **272**, 341 (2004).
- ¹¹S. W. Kang, Ph.D. dissertation, University of Florida, 2004.
- ¹²O. Kryliouk, M. Reed, T. Dann, T. Anderson, and B. Chai, *Mater. Sci. Eng., B* **59**, 6 (1999).
- ¹³I. Sayago, E. Terrado, E. Lafuente, M. C. Horillo, W. K. Maser, A. M. Benito, R. Navarro, E. P. Urriolabeita, M. T. Martinez, and J. Gutierrez, *Synth. Met.* **148**, 15 (2005).
- ¹⁴Y. Lu, J. Li, H. T. Ng, C. Binder, C. Partridge, and M. Meyyapan, *Chem. Phys. Lett.* **391**, 344 (2004).
- ¹⁵Q. Wan, Q. H. Li, Y. J. Chen, T. H. Wang, X. L. He, J. P. Li, and C. L. Lin, *Appl. Phys. Lett.* **84**, 3654 (2004).
- ¹⁶K. Keem, H. Kim, G. T. Kim, J. S. Lee, B. Min, K. Cho, M. Y. Sung, and S. Kim, *Appl. Phys. Lett.* **84**, 4376 (2004).
- ¹⁷Q. H. Li, Q. Wan, Y. X. Liang, and T. H. Wang, *Appl. Phys. Lett.* **84**, 4556 (2004).
- ¹⁸O. Kryliouk, H. J. Park, and T. Anderson (unpublished).
- ¹⁹K. D. Mitzner, J. Sternhagen, and D. W. Galipeau, *Sens. Actuators B* **93**, 92 (2003).
- ²⁰P. Mitra, A. P. Chatterjee, and H. S. Maiti, *Mater. Lett.* **35**, 33 (1998).
- ²¹H. L. Hartnagel, A. L. Dawar, A. K. Jain, and C. Jagadish, *Semiconducting Transparent Thin Films* (IOP, Bristol, 1995).
- ²²J. F. Chang, H. H. Kuo, I. C. Leu, and M. H. Hon, *Sens. Actuators B* **84**, 258 (1994).
- ²³E. A. Davis, S. F. J. Cox, R. L. Lichti, and C. G. Van de Walle, *Appl. Phys. Lett.* **82**, 592 (2003).